Title
The histone methyltransferase EZH2 is required for normal uterine development and function in mice

Journal
Biology of Reproduction, 101(2)

ISSN
0006-3363

Authors
Nanjappa, Manjunatha K
Mesa, Ana M
Medrano, Theresa I
et al.

Publication Date
2019-08-01

DOI
10.1093/biolre/ioz097

Peer reviewed

Biology of Reproduction, 2019, 101(2), 306–317
doi:10.1093/biolre/ioz097
Research article
Advance Access Publication Date: 14 June 2019

OXFORD

Research article

The histone methyltransferase EZH2 is required for normal uterine development and function in mice†

Manjunatha K. Nanjappa [1], Ana M. Mesa[1], Theresa I. Medrano [1], Wendy N. Jefferson[2], Francesco J. DeMayo[2], Carmen J. Williams [2], John P. Lydon[3], Ellis R. Levin [4,5] and Paul S. Cooke [1,*]

[1]Department of Physiological Sciences, University of Florida, Gainesville, Florida, USA; [2]Reproductive and Developmental Biology Laboratory, National Institute of Environmental Health Sciences, Research Triangle Park, North Carolina, USA; [3]Department of Molecular and Cellular Biology, Baylor College of Medicine, Houston, Texas, USA; [4]Division of Endocrinology, Department of Medicine, University of California-Irvine, Irvine, California, USA and [5]Department of Veterans Affairs Medical Center, Long Beach, Long Beach, California, USA

*__Correspondence:__ Department of Physiological Sciences, University of Florida, B3-6, Basic Science Building, PO Box 100144, Gainesville, FL 32610, USA. Tel: 35-2294-4008; Fax: 35-2392-8908; E-mail: paulscooke@ufl.edu

†__Grant support:__ This work was supported by NIH grants HD 088006, HD 087528 and PR015540 (to PSC). This work was also supported in part by the Intramural Research Program of the National Institutes of Health, National Institutes of Environmental Health Sciences, 1ZIAES102405 (to CJW).
Edited by Dr. Romana Nowak, PhD, University of Illinois Urbana-Champaign

Received 15 December 2018; Revised 26 April 2019; Accepted 6 June 2019

Abstract

Enhancer of zeste homolog 2 (EZH2) is a rate-limiting catalytic subunit of a histone methyltransferase, polycomb repressive complex, which silences gene activity through the repressive histone mark H3K27me3. EZH2 is critical for epigenetic effects of early estrogen treatment, and may be involved in uterine development and pathologies. We investigated EZH2 expression, regulation, and its role in uterine development/function. Uterine epithelial EZH2 expression was associated with proliferation and was high neonatally then declined by weaning. Pre-weaning uterine EZH2 expression was comparable in wild-type and estrogen receptor 1 knockout mice, showing neonatal EZH2 expression is ESR1 independent. Epithelial EZH2 was upregulated by 17β-estradiol (E2) and inhibited by progesterone in adult uteri from ovariectomized mice. To investigate the uterine role of EZH2, we developed a EZH2 conditional knockout (*Ezh2*cKO*)* mouse using a cre recombinase driven by the progesterone receptor (*Pgr*) promoter that produced *Ezh2*cKO mice lacking EZH2 in *Pgr*-expressing tissues (e.g. uterus, mammary glands). In *Ezh2*cKO uteri, EZH2 was deleted neonatally. These uteri had reduced H3K27me3, were larger than WT, and showed adult cystic endometrial hyperplasia. Ovary-independent uterine epithelial proliferation and increased numbers of highly proliferative uterine glands were seen in adult *Ezh2*cKO mice. Female *Ezh2*cKO mice were initially subfertile, and then became infertile by 9 months. Mammary gland development in *Ezh2*cKO mice was inhibited. In summary, uterine EZH2 expression is developmentally and hormonally regulated, and its loss causes aberrant uterine epithelial proliferation, uterine hypertrophy, and cystic endometrial hyperplasia, indicating a critical role in uterine development and function.

Summary Sentence

Loss of the histone methyltransferase EZH2 in the mouse uterus results in changes in uterine development and ovary-independent epithelial proliferation and ultimately causes infertility.

Key words: uterus, epigenetics, cell proliferation, mammary gland.

Introduction

Epigenetic regulation of gene expression is critical for tissue differentiation during development and exposure to exogenous hormones or endocrine disruptors can alter the epigenetic landscape in reproductive organs [1]. Histone methylation is an important mechanism of epigenetic gene regulation. Enhancer of zeste homolog 2 (EZH2) is a rate-limiting catalytic subunit of the polycomb repressive complex 2 (PRC2), a histone methyltransferase critical in histone modifications [2]. PRC2 represses gene transcription in target genes by trimethylating histone 3 at lysine 27 (H3K27me3), which induces transcriptional silencing [2].

Some evidence suggests that EZH2 is involved in normal uterine physiology as well as endometrial cancer and other diseases. Downregulation of EZH2 is critical for human uterine stromal cell decidualization [3]. Overexpression of EZH2 or EZH2 gain-of-function mutations occur frequently in endometrial [4–6], breast [7, 8], and prostate [9] cancer, as well as nonreproductive cancers [10]. Loss-of-function mutations in EZH2 are also associated with abnormal growth/cell proliferation [10].

Epithelial cells in endometriotic lesions in women express high EZH2 levels, suggesting a role in endometriosis pathogenesis [11]. Recent results have indicated that EZH2 might be involved in the etiology of human uterine leiomyomas [12–14]. Furthermore, developmental exposure of rats to environmental estrogens induces adult uterine leiomyomas, potentially through EZH2 [15]. Similarly, estrogen treatment in utero increases mammary EZH2 in rodents and was linked to increased breast cancer risk in adult women [16, 17], and loss of EZH2 alters mammary development in mouse models [18–20].

Exposure of neonatal mice to DES altered uterine levels of the phosphorylated (inactive) form of EZH2, histone marks, and expression of key uterine proteins [1, 21, 22]. Estrogen effects may be mediated through membrane ESR1, which activates the phosphotidylinositol-3-kinase (PI3K)/AKT pathway and phosphorylates and represses EZH2 [22, 23]. Furthermore, EZH2 expression is induced by estrogens (e.g. DES, BPA) in mammary glands potentially through estrogen response elements (ERE) in the EZH2 gene promoter [16].

Despite the potential role of EZH2 in uterine physiology/pathology and the observation that early estrogen exposure induces uterine epigenetic alterations, information regarding uterine EZH2 expression and its regulation was minimal. Likewise, the effect of loss of EZH2 on uterine development/function was unknown. In this study, we analyzed EZH2 expression and hormonal regulation by estrogen and ESR1 in postnatal mouse uteri.

Initial work [24] indicated that global knockout of *Ezh2* caused embryonic lethality, reflecting critical EZH2 roles in development. Subsequent work therefore focused on developing conditional *Ezh2* knockouts in particular cell/tissue types. Conditional *Ezh2* knockouts in mammary epithelial stem cells, early mesenchyme, heart, cerebellum, intestine, liver, and other tissues [20, 25–29] have been reported. In this study, we also used mice expressing Cre recombinase under the control of the *Pgr* promoter in conjunction with floxed *Ezh2* genes to produce conditional *Ezh2*cKO mice lacking EZH2 in PGR-expressing tissues such as uterus, mammary gland, cervix, vagina, oviduct, and some brain regions. These *Ezh2* conditional knockout (*Ezh2*cKO*)* mice were used to investigate EZH2's role in uterine development and function.

Materials and methods

Animals and animal care

The WT, estrogen receptor 1 knockout (*Esr1*KO; gift from Drs. Pierre Chambon and Andrée Krust, Institut de Génétique et de Biologie Moléculaire et Cellulaire, Illkirch, France), and nuclear-only estrogen receptor (NOER) mice, which express nuclear ESR1 but lack membrane ESR1 [30], were on mixed C57BL/6 and 129SV backgrounds. The *Esr1*KO and NOER mice used were generated and genotyped as described previously [31, 32].

Transgenic mice expressing Cre recombinase under control of the *Pgr* promoter [33] were also on mixed C57BL/6 and 129SV backgrounds. These mice were originally obtained from Drs. Franco DeMayo (NIEHS, Research Triangle Park, NC) and John Lydon (Baylor College of Medicine, Houston, TX). Female homozygous *Ezh2* floxed mice (stock #022616) in which the *Ezh2* coding region is flanked by two loxP sites in both *Ezh2* alleles were purchased from Jackson Laboratory (Bar Harbor, ME) [34].

Mice were housed in standard polycarbonate/polysulfone cages at 25°C with 12L:12D cycles and given water and a standard rodent diet ad libitum. All animal experiments were approved by the IACUC of the University of Florida and conducted in accordance with the NIH Guide for the Care and Use of Laboratory Animals.

Generation of Ezh2cKO mice

Transgenic *Pgr*-Cre mice were bred with homozygous floxed *Ezh2* mice. Male and female offspring expressing *Pgr*-Cre and heterozygous for floxed *Ezh2* ($Pgr^{wt/Cre}$, $Ezh2^{+/flox}$) were then crossed to obtain males that expressed *Pgr*-Cre and were homozygous for floxed *Ezh2* ($Pgr^{wt/Cre}$, $Ezh2^{flox/flox}$); these males were normally fertile. These males were then mated with $Pgr^{wt/wt}$, $Ezh2^{flox/flox}$ females. Half of the resulting female offspring had a $Pgr^{wt/Cre}$, $Ezh2^{flox/flox}$ genotype, resulting in deletion of *Ezh2* in *Pgr*-expressing tissues. The remaining half were $Pgr^{wt/wt}$, $Ezh2^{flox/flox}$, which served as experimental WT controls.

Genotyping

Mice were genotyped using tail genomic DNA with the REDExtract-N-Amp Tissue PCR kit (Sigma, St. Louis, MO) according to the manufacturer's instructions. The *Ezh2*cKO mice ($Pgr^{wt/Cre}$, $Ezh2^{flox/flox}$) expressed Cre and two floxed *Ezh2* genes, whereas WT control animals ($Pgr^{wt/wt}$, $Ezh2^{flox/flox}$) expressed floxed *Ezh2* but no Cre. Genotyping for *Pgr*-Cre and floxed *Ezh2* was performed at weaning by multiplex PCR on genomic DNA using primers specific for *Pgr* (Primer 1; 5′-TATACCGATCTCCCTGGACG -3′, Primer 2; 5′-ATGTTTAGCTGGCCCAAATG-3′, Primer 3; 5′-CCCAAAGAGACACCAGGAAG-3′ as described previously [35] or floxed *Ezh2* (Primer 1; 5′-CATGTGCAGCTTTCTGTTCA-3′

Primer 2; 5′-CACAGCCTTTCTGCTCACTG-3') (Jackson Laboratory, stock# 022616). PCR was performed by denaturing DNA at 94°C for 3 min, followed by 30 amplification cycles (94°C for 45 s, 60°C for 45 s, 72°C for 90 s) and a final extension step at 72°C for 5 min. The final PCR reaction mixture was run on 1–2% agarose gel using ethidium bromide to visualize PCR products of 500 bp for *Pgr*-Cre and 300 bp for floxed *Ezh2*.

Developmental expression of uterine EZH2

Uteri from WT mice ranging from postnatal day (PND) 6 to 60 were immunostained for EZH2. To determine whether EZH2 expression was ESR1 dependent, EZH2 immunostaining was compared in WT and *Esr1*KO mice ranging from neonatal to adult. The PND 35 and 60 mice used were in proestrous when tissues were harvested.

Immunohistochemistry was performed as described previously [31, 32]. Briefly, uteri were immersion fixed in 10% neutral-buffered formalin for at least 48 h. Fixed uteri were paraffin embedded, sectioned at 5–6 μm, deparaffinized, and rehydrated. Antigen retrieval was performed in 10 mM boiling sodium citrate buffer (pH 6.0) for 18 min and cooled to ambient temperature. Endogenous peroxidase activity was quenched by incubation with 0.6% H_2O_2 in methanol for 20 min. Slides were incubated with one of the primary antibodies overnight at a 1:1000 dilution using rabbit monoclonal IgG for EZH2 (Antibody ID AB 10694683; catalog #5246; Cell Signaling Technology, Danvers, MA) and MKI67 (Antibody ID AB 302459; catalog #ab16667; Abcam Inc.). Binding of primary antibody to the protein of interest was localized using the Vectastain ABC (Kit Catalog #PK-4000, Vector Laboratories, Burlingame, CA) and DAB Substrate Kit (Vector Laboratories), according to the manufacturer's instructions. Sections were counterstained with Gill hematoxylin (catalog no. 245–654; Fisher Scientific). Negative controls were processed without primary antibody and counterstained as above.

Hormonal regulation of uterine EZH2 expression

To test E2 and P4 effects on uterine EZH2 expression, PND 60 WT control females were ovariectomized. Two weeks later, they were injected once daily for 3 days with (a) oil vehicle (0.2 ml); (b) vehicle for 2 days, followed by one day of E2 (10 ng/g BW in oil); or (c) 2 days of P4 (40 μg/g BW in oil vehicle) followed by 1 day of P4 (40 μg/g BW) + E2 (10 ng/g BW). Uteri were collected 24 h later and processed either for immunostaining (EZH2, MKI67) or EZH2 western blotting.

For EZH2 western blotting, uterine tissue was lysed in T-PER lysis buffer. Proteins were separated by SDS-PAGE and transferred to nitrocellulose membrane. Blots were probed with the EZH2 antibody used for immunohistochemistry (1:1000) followed by goat anti-rabbit horseradish peroxidase conjugate secondary antibody (BioRad, Hercules CA) and incubation in chemiluminescent reagents (see Supplemental Table S1 for complete antibody list). Signal was then captured using a LI-COR C-DiGit Chemiluminescence Western Blot Scanner. Actin was used as a loading control, and was visualized using antibody #sc-1616 (Antibody ID AB 630836) from Santa Cruz Biotechnology (Santa Cruz, CA) at a dilution of 1/2000. Comparative intensity of the EZH2 bands was measured by densitometry using NIH Image J software.

To determine whether membrane ESR1 is required for full stimulatory estrogen effects on EZH2 expression, female WT and NOER [30] mice were ovariectomized at PND 60. Two weeks later, half were given one injection of E2 in oil (10 ng/g BW) and half vehicle alone. Uteri were removed 24 h later, fixed, sectioned, then used for EZH2 immunohistochemistry. To compare EZH2 immunostaining in E2-treated WT and NOER uteri, an H-score for staining intensity was calculated by assessing the extent of nuclear immunoreactivity in 100 epithelial cells. The H-score was the sum obtained by multiplying the percentage of strongly stained nuclei by 3 and adding the percentage of moderately stained nuclei times 2 plus the percentage of weakly stained nuclei; nuclei showing no staining received a value of zero, and resultant scores ranged from 0 to 300.

Analysis of EZH2, H3K27me3, and H3K27ac expression in Ezh2cKO mice

Uterine and mammary gland EZH2 expression was examined by immunostaining adult WT and *Ezh2*cKO tissues to confirm EZH2 deletion in *Ezh2*cKO tissues. To determine when EZH2 was deleted in *Ezh2*cKO tissues, we performed western analysis on WT and *Ezh2*cKO uteri at PND 6 and 15.

To determine if loss of EZH2 altered histone methylation and/or acetylation, histones were purified from approximately 20 mg of uterine tissue from individual PND 60 WT and *Ezh2*cKO mice, as previously described [36]. Cytoplasmic and nuclear fractions were isolated first using the NE-PER kit (Thermo Fisher) following the manufacturer's directions. After removing the nuclear fraction, 0.4 N H_2SO_4 was added to the pellet for 30 min on ice. Samples were centrifuged, supernatant was removed to a new tube, and acetone was added to precipitate the histones overnight at –20°C. Samples were centrifuged at maximum speed at 4°C for 15 min. Acetone was removed and the pellet was resuspended in water. Histones (2 μg) were loaded onto 12% SDS-PAGE gels (Bio-Rad). For gel staining, the gel was rinsed with dH_2O, stained with Simply Blue (Thermo Fisher) for 1 h, and rinsed with dH_2O. For immunoblotting, histones were transferred to PVDF membrane. Immunoblotting was performed as previously described [21, 22] with anti-H3K27ac (Active Motif), anti-H3K27me3 (Antibody ID 449502; Abcam), or anti-H3 (Antibody ID 732917, Abcam), all at a 1:1000 dilution, in 5% milk in TBS-T as the primary antibodies and donkey anti-rabbit (Antibody AB 10015282, Jackson Immunolabs) diluted 1:25,000 in 1% milk in TBS-T as the secondary antibody. Bands were visualized with Super Signal West Femto (Thermo Fisher) and imaged using the Chemi Doc Touch Imaging System (Bio-Rad).

Uterine and mammary gland morphology and histology in Ezh2cKO mice

Whole mount images were taken of freshly dissected *Ezh2*cKO and WT uteri at PND 22, 60, and 180. Uteri were then weighed, fixed, then sectioned and stained with hematoxylin and eosin, or immunostained for FOXA2, a uterine gland marker [37]. Whole mounts of PND 60 *Ezh2*cKO and WT mammary glands from ($Pgr^{+/+}$, $Ezh2^{flox/flox}$) were prepared as previously described [38]. Briefly, fourth mammary glands were collected and spread on glass slides. Mammary glands were fixed with Carnoy fixative for 24 h, rehydrated, and stained overnightwith carmine alum. Stained mammary glands were dehydrated, cleared overnight with Hemo-D, mounted using Permount, and photographed using a dissection microscope-mounted camera.

Hormonal regulation of uterine weight and cell proliferation

To investigate EZH2's role in uterine estrogen signaling, adult WT and *Ezh2*cKO mice were ovariectomized at PND 60. Two weeks later, mice were given oil vehicle or E2 (0.2–10 ng/g BW, ip). After

24 h, uteri were collected, weighed, and immunostained for MKI67; labeling indices (LI; labeled/total cells) were determined in luminal epithelium.

Reproduction in Ezh2cKO female mice

To assess fertility in *Ezh2*cKO female mice, *Ezh2*cKO and WT females at various ages were housed with proven breeder males for 30 days or until pregnancy occurred, and pregnancy success was recorded. For mice that became pregnant, litter size and percentage of live pups born that survived to weaning in each litter were also recorded.

To determine whether *Ezh2*cKO females cycled, mated, and implanted normally, we performed cytological examination of vaginal smears of *Ezh2*cKO mice (n = 12) that ranged from 1.5 to 5 months of age and WT mice (n = 10) that ranged from 2.5 to 6 months of age. Six of the *Ezh2*cKO mice were monitored through two to three cycles, while the remaining mice were monitored through five cycles. All mice were then mated with proven breeder males, and monitored for a postcoital vaginal plug. Detection of the vaginal plug was designated as gestation day (GD) 0.5. Mice were sacrificed at GD 7.5 or 8.5, and uteri were examined for implantation sites and hyperemia. Uteri of WT and *Ezh2*cKO mice that had implantation sites and those of *Ezh2*cKO mice that did not exhibit implantation sites were processed for routine histology to determine whether the decidual response occurred in these uteri and was histologically normal. At necropsy, the number of corpora lutea in both pregnant and nonpregnant WT and *Ezh2*cKO mice was determined, and this was compared with the number of implantation sites in pregnant animals.

Statistical analysis

Data were analyzed using the Student *t*-test to identify significant differences between two groups. When comparing more than two groups, one-way analysis of variance (ANOVA) followed by the Dunnett multiple comparisons test was used. Chi-square tests were used to assess fertility differences between groups. Differences were considered significant at $P < 0.05$. Statistical analysis was performed with Graph Pad Prism 6.0 (Graph Pad Software, Inc., San Diego, CA).

Results

Uterine EZH2 expression during development and adulthood

Expression of EZH2 expression was high in both uterine epithelium and stroma of PND 6 WT and *Esr1*KO mice (Figure 1). EZH2 expression was decreased in uterine stroma and epithelium of PND 22 WT and *Esr1*KO uteri compared to earlier ages. In WT mice in proestrus at PND 35 and 60, significant epithelial EZH2 expression was seen; conversely, EZH2 expression was lower during diestrus at these ages (data not shown). In contrast to the similar expression between WT and *Esr1*KO uteri from PND 6–22, EZH2 expression in *Esr1*KO uteri at PND 35 and 60 was lower than WT.

High uterine EZH2 expression (Figure 1) in WT and *Esr1*KO uteri at PND 6 corresponded with high epithelial proliferation in these uteri (Figure 1). Uterine epithelial proliferation reached a nadir at PND 22, when EZH2 expression in both genotypes was also lower than PND 6. After puberty, the relatively high EZH2 uterine epithelial expression in proestrous WT mice was associated with significant proliferation (as indicated by MKI67 staining). The lower EZH2 expression in epithelium of *Esr1*KO uteri at PND 35 and 60 was associated with lower proliferation in these cells at those ages, as we reported previously [32].

Uterine expression of EZH2 is regulated by estrogen and progesterone

In vehicle-treated ovariectomized WT females, immunostaining for EZH2 and MKI67 (cell proliferation marker) was low (Figure 2A). As expected, E2 sharply increased epithelial EZH2 and MKI67 expression. Pretreatment for 2 days with progesterone sharply diminished stimulatory E2 effects on epithelial EZH2 and MKI67 expression; however, this treatment increased stromal EZH2 expression. Western blotting of EZH2 (Figure 2B and C) confirmed immunohistochemistry results, and it is likely that EZH2 expression in response to P4 + E2 in the Western blot predominantly reflects stromal EZH2 expression.

Expression of EZH2 is reduced in NOER uteri

Previous results suggested that estrogen effects on EZH2 may be mediated through the fraction of ESR1 that is localized to the cell membrane [15, 22]. To determine whether membrane ESR1 is required for estrogen-stimulated EZH2 expression, we used NOER mice that lack membrane ESR1 despite expressing normally functional nuclear ESR1 [30]. Expression of EZH2 in uterine epithelium of vehicle-treated ovariectomized NOER and WT mice was low. Treatment with E2 induced strong increases in EZH2 staining in epithelium of ovariectomized WT mice, but these increases were attenuated in E2-treated ovariectomized NOER females (Figure 3). The H-score data for these various groups confirmed these results and indicated that uterine epithelial staining intensity for WT treated with E2 was greater than for NOER mice treated with E2 (287 ± 6 and $225 + 15$, respectively; $P = 0.01$ and n = 4 for both groups). The H-scores for the uterine epithelium of WT or NOER mice treated with vehicle (66 ± 22, n = 4 and $112 + 12$, n = 3, respectively) were not different ($P \geq 0.05$), and the H-score was significantly higher for the E2 vs oil group in both genotypes ($P \leq 0.001$) These data, combined with the lack of E2 stimulation of EZH2 in *Esr1*KO uteri, show that membrane ESR1 is necessary for full stimulatory E2 responses in WT mice.

Uterine and mammary EZH2 expression in Ezh2cKO mice

EZH2 immunostaining in adult (PND 60) *Ezh2*cKO uteri indicated that EZH2 was not expressed in luminal or glandular epithelium (Figure 4A), although some stromal expression was evident. EZH2 immunostaining in PND 60 *Ezh2*cKO mammary glands was not seen (data not shown). Western analysis of uterine EZH2 expression at PND 6 and 15 (Figure 4B) indicated that EZH2 expression in *Ezh2*cKO uteri was decreased compared to WT at PND 6 and 15.

To determine the consequences of loss of uterine EZH2 on histone modifications, we examined global levels of H3K27me3 and H3K27ac. Western analysis of H3K27me3 in *Ezh2*cKO uteri showed that expression was down sharply compared to WT controls (Figure 4C). Conversely, H3K27ac showed a trend toward an increase in *Ezh2*cKO vs WT uteri, although this did not reach statistical significance likely due to sample variability. This resulted in a sharply decreased H3K27me3/H3K27ac ratio in *Ezh2*cKO vs WT uteri (Figure 4C).

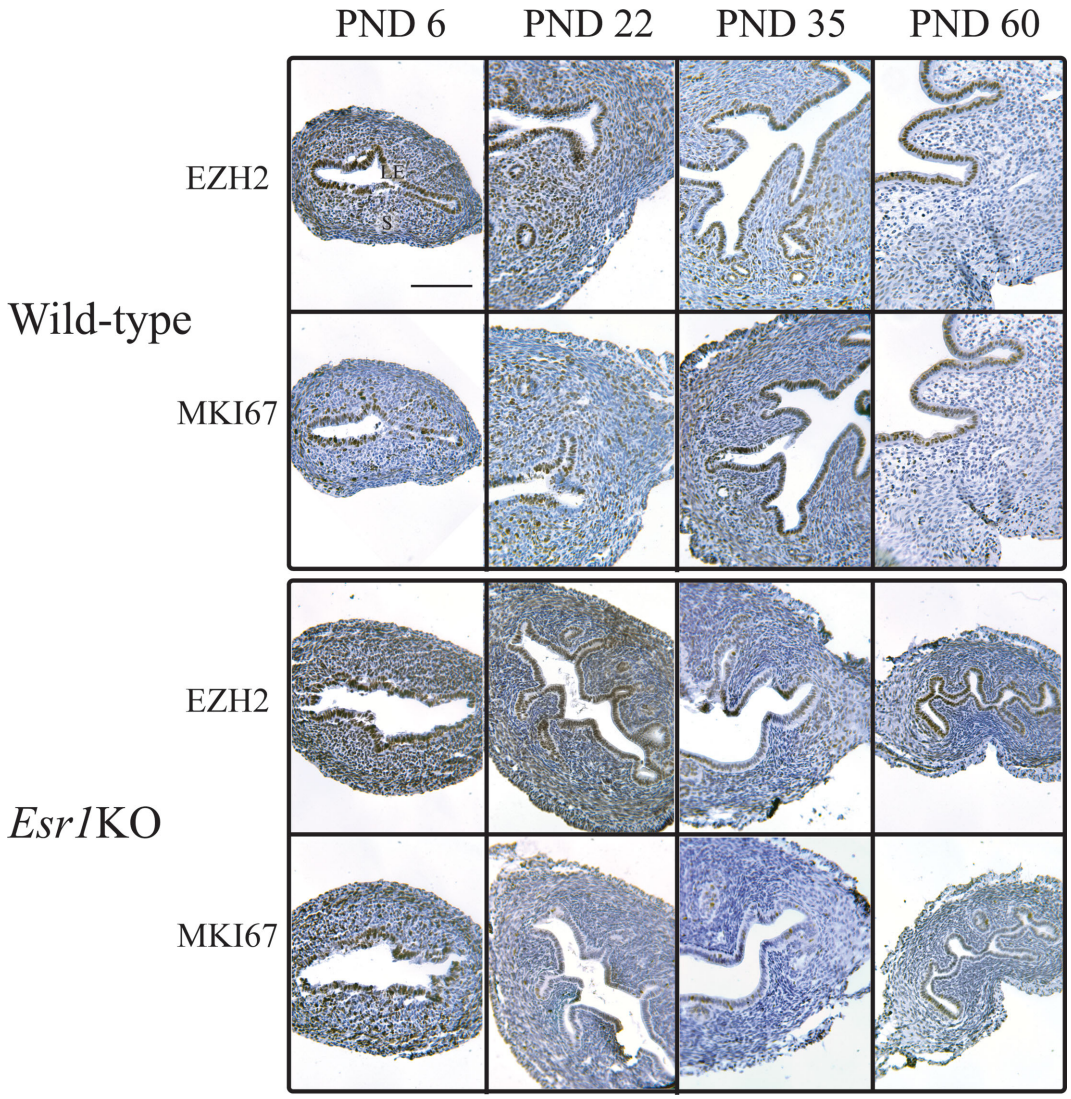

Figure 1. Postnatal mouse uterine EZH2 expression is developmentally regulated and correlated with epithelial cell proliferation. Uterine EZH2 and MKI67 expression were visualized by immunohistochemistry of serial sections in WT and *Esr1*KO mice at 6–60 days. Luminal epithelial (LE) and stromal (S) EZH2 and MKI67 expression showed striking changes during development. In *Esr1*KO mice, EZH2 expression was comparable to WT mice at PND 6, but lower than WT during and after puberty. All images are at the same magnification; magnification bar = 0.3 mm. A n of 3–5 animals from at least three litters was used for all groups.

Uterine size and weight in Ezh2cKO mice

The *Ezh2*cKO uteri were increased in weight (Figure 5A) and size (Figure 5B) compared to WT. Significant uterine weight increases were detected at PND 22, the earliest age at which uterine weight was measured (Figure 5A). By PND 60 uterine weights in *Ezh2*cKO mice were approximately double that of WT, and by PND 180, *Ezh2*cKO uterine weights were 3.8-fold that of WT. Whole mounts of *Ezh2*cKO uteri (Figure 5B) showed age-dependent organomegaly compared to WT. By PND 120, whole mounts of *Ezh2*cKO uteri showed numerous light, translucent areas throughout both horns (Figure 5B); these translucent areas (Figure 5C) represented large cysts that often contained inflammatory cell infiltrates. Uterine changes in *Ezh2*cKO mice occurred despite comparable body weights in WT and *Ezh2*cKO mice at all ages (data not shown). Staining with FOXA2 (Figure 5D), a specific marker for uterine glands, showed that ovariectomized *Ezh2*cKO uteri had large increases in gland number relative to WT at PND 74 (Figure 5D); gland number per uterine cross section in WT and *Ezh2*cKO mice was 20.3 ± 1.4 and 49.7 ± 4.6, respectively (n = 3 for both groups; $P = 0.004$).

Estrogen effects on uterine weight and epithelial proliferation in Ezh2cKO mice

In adult ovariectomized mice, E2 produced dose-responsive increases in uterine weight and epithelial proliferation in WT and *Ezh2*cKO females. The *Ezh2*cKO mice exhibited increased uterine weight compared to their WT counterparts in both the oil-treated and E2 treatment groups. Uterine weights in oil-treated WT females were less than those in *Ezh2*cKO females, and similar increases were seen in *Ezh2*cKO and WT uteri with all E2 doses (data not shown). Epithelial proliferation was low in oil-treated ovariectomized WT mice, as anticipated (Figure 6A and B). However, uterine epithelial

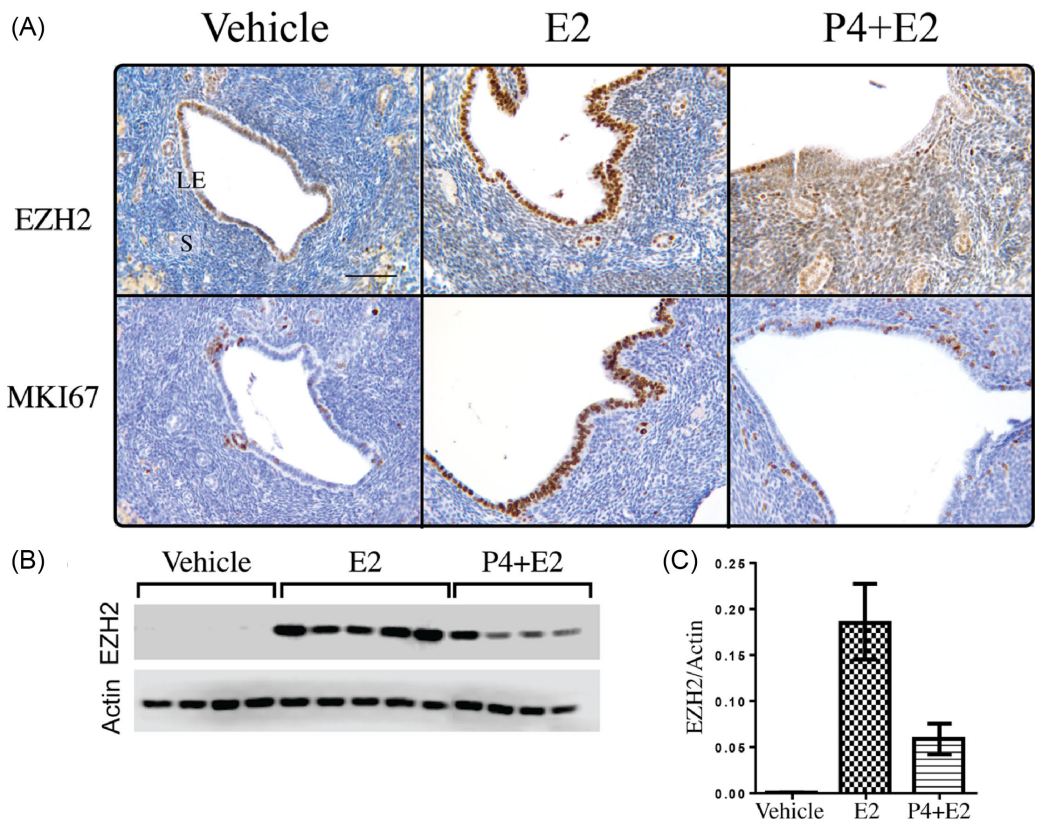

Figure 2. Regulation of EZH2 expression by E2 and P4 in adult uteri. Adult WT females were ovariectomized and were treated 2 weeks later with (a) 3 days of oil vehicle, (2) 2 days of oil and on third day E2 (10 ng/g BW), or (3) 2 days of P4 (40 μg/g BW) and on the third day P4 (40 μg/g) and E2 (10 ng/g). Uteri were collected and immunostained for EZH2 and MKI67. (A) EZH2 expression was stimulated by E2 in luminal epithelium (LE), but not stroma (S), while P4 inhibited E2-induced epithelial EZH2 increases but increased stromal EZH2. Increased epithelial EZH2 expression was associated with increased proliferation. All images are at the same magnification; magnification bar = 0.1 mm. (B) Western blot of EZH2 in adult WT mice given E2 or E2 + P4, and (C) quantitation of western results in (B). All values were significantly ($P \leq 0.01$) different. A n of 4–5 was used for all groups for both immunohistochemistry and western blotting.

proliferation in oil-treated ovariectomized *Ezh2*cKO females was about four-fold greater that in WT controls (Figure 6A and B), with uterine luminal epithelium showing substantial proliferation even in the absence of ovarian and exogenous E2. In addition, vehicle-treated *Ezh2*cKO mice showed striking increases in both luminal and glandular epithelial proliferation compared to WT mice, and gland number/uterine cross section was increased (Figure 6A). In mice given 0.2 ng/g BW E2, epithelial proliferation was also greater in *Ezh2*cKO than WT mice, but maximal proliferation was obtained at 10 ng/g BW E2 and was comparable in WT and *Ezh2*cKO mice.

Fertility and mammary gland development in Ezh2cKO mice

Female *Ezh2*cKO mice were initially fertile, but they showed subfertility with advancing age (Figure 7A). By 8 months of age, *Ezh2*cKO females were completely infertile, even though WT females at this age remained maximally fertile.

Although young *Ezh2*cKO females often produced litters, litter size was smaller than in WT mice over their reproductive lifespan (Table 1). In addition, reproductive problems such as dystocia sometimes occurred in *Ezh2*cKO females, but not in WT controls. Pup survival was also reduced in litters from *Ezh2*cKO compared to WT mice. In this model of *Ezh2* conditional deletion, the mammary gland of *Ezh2*cKO females has reduced EZH2 due to PgR expression in this tissue. We hypothesized that a defect in mammary gland function could result in decreased pup survival. Whole mounts of WT and *Ezh2*cKO mammary glands (Figure 7B) revealed reduced epithelial branching and terminal mammary end bud numbers in *Ezh2*cKO compared to WT mice. Thus, in contrast to their uterine organomegaly, mammary glands of *Ezh2*cKO mice were underdeveloped. This suggested potential impacts on milk production and pup survival so we measured body weight in WT and *Ezh2*cKO pups. Although fewer pups of *Ezh2*cKO mothers survived to weaning, remaining pup weights were not reduced at PND 10 or 20 (data not shown), and post-weaning pup survival was unaffected by maternal genotype. This indicates that despite their underdeveloped mammary glands, lactation was sufficient to allow normal growth of the smaller litters from *Ezh2*cKO dams.

Ovarian and uterine function in Ezh2cKO mice

All female WT and *Ezh2*cKO mice cycled normally. Cycle duration in WT and *Ezh2*cKO mice was comparable, and the cycles in *Ezh2*cKO mice that did not subsequently become pregnant were indistinguishable from WT and *Ezh2*cKO mice that did become pregnant after mating.

Following co-housing with a proven breeder male, 11/12 *Ezh2*cKO mice had an identifiable copulation plug. Overall, 7/12 of the *Ezh2*cKO and 8/10 of the WT mice became pregnant, as

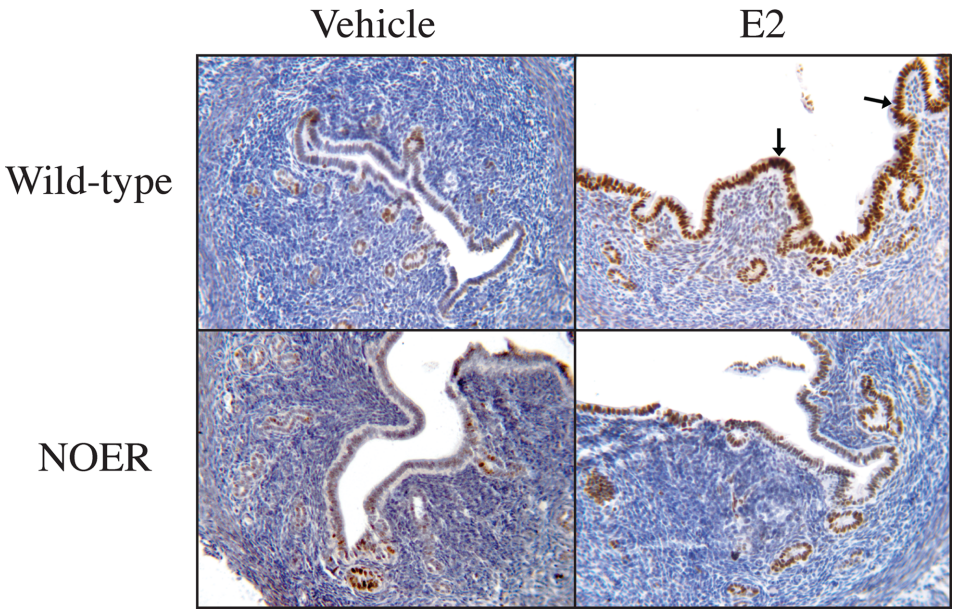

Figure 3. Expression of EZH2 in response to E2 in uterine epithelium is reduced in NOER mice. Adult ovariectomized WT and NOER females mice were given oil or E2 (10 ng/g BW). Uteri were collected 24 h later, fixed, and immunostained for EZH2. Expression of EZH2 was minimal in vehicle-treated WT and NOER uteri. There was a strong stimulatory effect of E2 on EZH2 expression in luminal and glandular epithelium in WT mice as shown by intense brown staining in the epithelium (arrows), but this E2 effect was attenuated in NOER mice. All images are at the same magnification; magnification bar = 0.1 mm. The n = 7 for each treatment and genotype.

judged by the presence of implantation sites at GD 7.5 or 8.5. The *Ezh2*cKO mice that became pregnant were on average 3.1 months of age at mating, while *Ezh2*cKO mice that did not were initially on average 3.8 months of age at mating. Pregnant WT mice (average age at mating = 4.1 months; n = 8) had an average of 8.3 ± 0.7 corpora lutea at necropsy, and these animals had 7.8 ± 0.5 implantation sites. In pregnant *Ezh2*cKO mice (n = 7), there were 8.6 + 0.7 corpora lutea, and these mice had 8.3 + 0.5 implantation sites; these values were not different from those in WT mice ($P \geq 0.05$). Nonpregnant *Ezh2*cKO mice (n = 5) had no evidence of implantation sites, but they had 6.4 + 0.7 corpora lutea; corpora lutea number did not differ from pregnant WT or *Ezh2*cKO mice ($P \geq 0.05$). Hyperemia was present in all pregnant uteri from both WT and *Ezh2*cKO mice, and hyperemia was also apparent in GD 7.5 or 8.5 *Ezh2*cKO mice that did not become pregnant. Histological examination of implantation sites of both pregnant WT and *Ezh2*cKO mice showed the presence of large decidualized stromal cells (data not shown), while decidualization was absent in nonpregnant *Ezh2*cKO mice.

Discussion

Our results show that EZH2 was highly expressed in neonatal uteri, especially in the epithelium, then declined with age. Uterine epithelial EZH2 expression correlated with epithelial proliferation. This was apparent both neonatally, when uterine epithelial proliferation and EZH2 expression were maximal, and during/after puberty, when there were increases in uterine epithelial proliferation and EZH2 expression in WT compared to *Esr1*KO mice.

Despite the correlation with epithelial proliferation, pre-weaning EZH2 expression does not require ESR1. This is shown by similar EZH2 expression and age-related decreases in WT and *Esr1*KO mice from the neonatal period to weaning. At and after puberty, uterine epithelial proliferation in *Esr1*KO mice was low [31, 32], and this correlated with low uterine epithelial EZH2 expression in these mice. Thus, ESR1 is dispensable for pre-weaning EZH2 expression, but loss of ESR1 is associated with lower EZH2 expression later when uterine epithelium becomes dependent on E2/ESR1 for proliferation.

The developmental pattern of EZH2 expression in uterine epithelium suggests that E2 may be a regulator of EZH2, and our data demonstrated that estrogen stimulates epithelial EZH2 expression in uteri of ovariectomized mice. Previous work in Eker rats [15, 22] demonstrated that DES or other estrogens increase the phosphorylated (p-EZH2), active EZH2 form in uterus, although total EZH2 was decreased at 6 h after estrogen treatment. Thus, our results are the first showing that E2 stimulates uterine EZH2 in pubertal and juvenile mouse uteri, although earlier results from Grimaldi et al. [3] showing higher levels of uterine EZH2 in the proliferative phase of the human endometrium suggested this possibility. Although E2 treatment stimulates EZH2 expression, it is unclear whether this is direct or indirect. The EZH2 gene contains an ERE [16], suggesting potential direct regulation of EZH2 by E2. However, EZH2 is similarly expressed in epithelium of neonatal *Esr1*KO uteri, suggesting that induction of proliferation triggers EZH2 expression. Thus, E2 stimulation of epithelial proliferation may increase EZH2 indirectly, rather than directly. Further investigations into the mechanism of E2 effects on EZH2 are needed to distinguish between these two possibilities.

In NOER mice previously used to demonstrate membrane ESR1 roles in female [30] and male [31, 32] reproduction, we found that stimulatory E2 effects on EZH2 expression seen in WT mice were attenuated. These data showing that membrane ESR1 is required for full EZH2 expression are consistent with previous results that membrane EZH2 is necessary for full E2 effects.

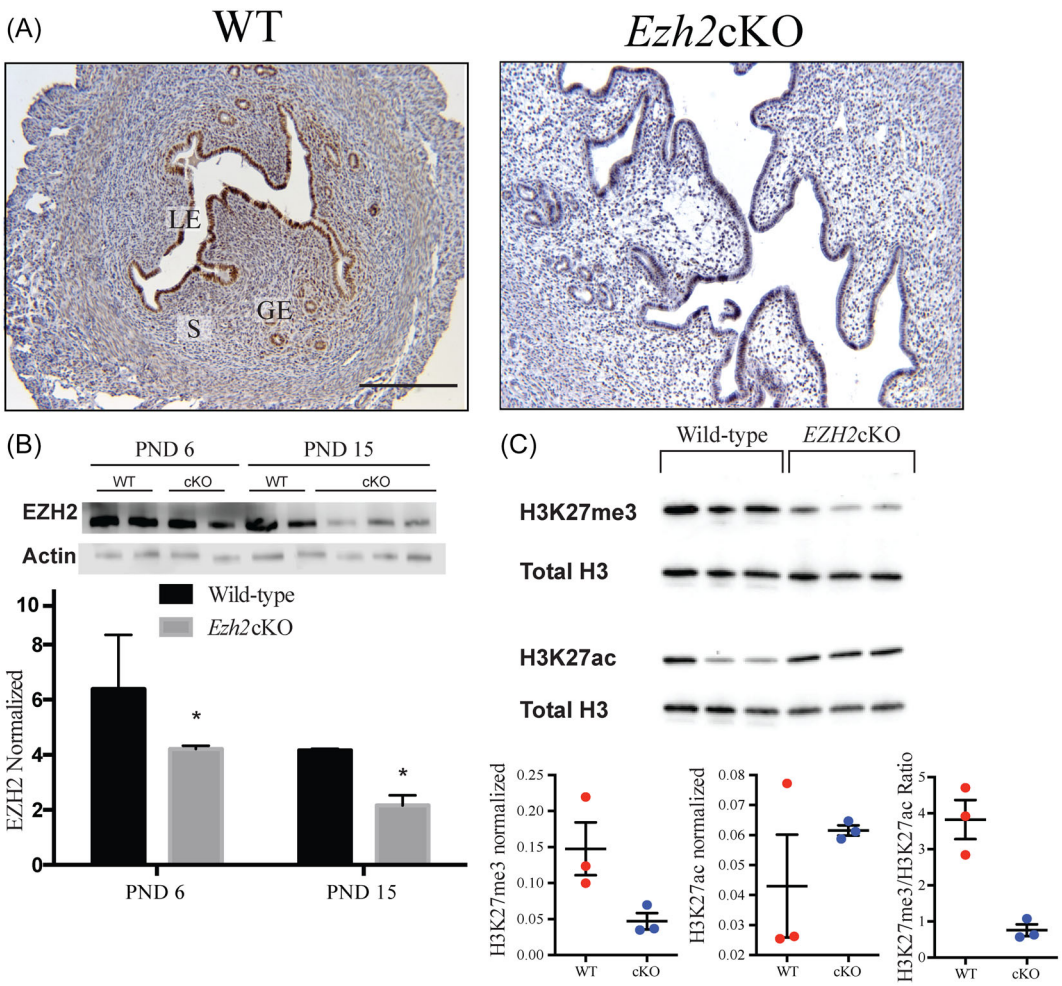

Figure 4. Uterine expression of EZH2, H3K27me3, and H3K27ac in WT and *Ezh2*cKO mice. (A) Adult (PND 60) WT uteri showed robust EZH2 staining in luminal epithelium (LE), glandular epithelium (GE), and stroma (S). Conversely, EZH2 was deleted in *Ezh2*cKO epithelium, although some stromal cells were EZH2-positive. Both images are the same magnification; magnification bar = 0.3 mm. The n = 4–5 for the WT and *Ezh2*cKO uteri. (B) Western blot (left) and quantitation (right) of EZH2 in PND 6 and 15 WT and *Ezh2*cKO uteri, normalized against actin. In *Ezh2*cKO uteri, EZH2 expression was significantly reduced at PND 6 and 15 but remained demonstrable in both ages. The n = 4 for WT uteri and n = 5 for *Ezh2*cKO uteri. (C) Western blot (left) of H3K27me3 and H3K27ac in uteri from intact adult WT and *Ezh2*cKO mice, both normalized against total uterine H3. The individual values for H3K27me3, H3K27ac, and the H3K27me3/H3K27ac ratio for each of the three WT and *Ezh2*cKO uteri are shown in the three graphs in the right panel. Uterine H3K27me3 in *Ezh2*cKO mice was reduced ($P \leq 0.05$) compared to WT. Conversely, H3K27ac in *Ezh2*cKO uteri showed a trend toward an increase compared to WT ($P = 0.137$), and the H3K27me3/H3K27ac ratio was approximately five-fold greater ($P \leq 0.05$) in WT compared to *Ezh2*cKO uteri. * = different than WT at $P \leq 0.05$.

Progesterone, which blocks mitogenic E2 effects on epithelium, sharply decreased uterine epithelial EZH2, consistent with other inhibitory progesterone effects on E2 actions in uterine epithelium. Conversely, P4 + E2 stimulated stromal EZH2 expression, showing that this treatment has opposite effects in different uterine compartments. A regimen of P4 + E2 stimulates proliferation of stromal cells, and EZH2 expression in stromal cells from mice given P4 + E2 may be an early response to this mitogenic stimulus. A 3-day E2 + P treatment is typically given to induce proliferation of stromal cells, and use of only one P4 + E2 injection here likely explains the low stromal MKI67 expression in E2 + P treated uteri even though they have been exposed to a hormonal regimen that is ultimately mitogenic if administered for a longer period of time.

Our results indicate that EZH2 was successfully deleted in uterine epithelium and in some but not all uterine stromal cells in *Ezh2*cKO mice. Uterine endothelial cells do not express *Pgr* (DeMayo, unpublished), and these cells, along with white blood cells, may still express EZH2 in *Ezh2*cKO uteri. Uterine PGR expression occurs as early as PND 3 [39], and our results indicate that decreased EZH2 expression is seen at PND 6 and 15. Thus, uterine EZH2 excision occurs during early postnatal life. Although there are histological and functional changes in *Ezh2*cKO adult uteri, initial adenogenesis, smooth muscle differentiation, and maturational events such as declining epithelial proliferation between birth and puberty occurred normally in *Ezh2*cKO uteri. Thus, loss of uterine EZH2 in *Ezh2*cKO mice does not alter initial uterine development.

Uterine H3K27me3 is down sharply in adult *Ezh2*cKO mice, consistent with EZH2's critical role in histone methylation. However, uterine H3K27me3 is still present, which may reflect persistence of uterine H3K27me3 laid down prior to neonatal *Ezh2* excision and

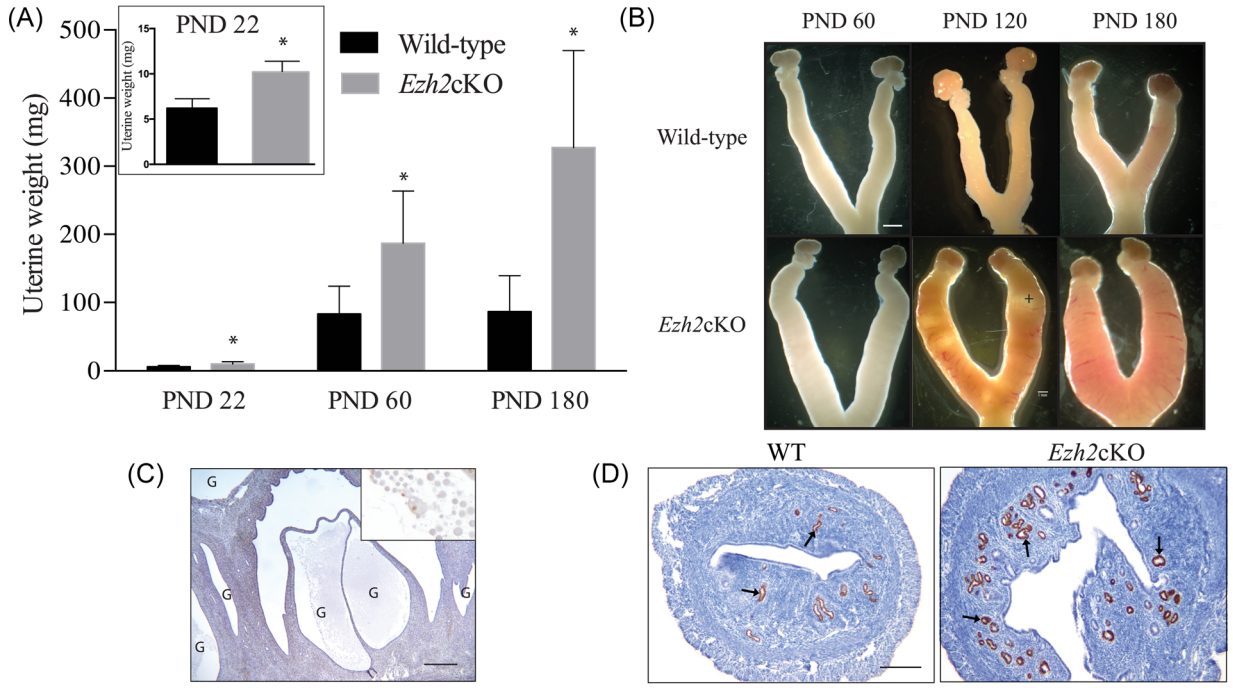

Figure 5. Loss of EZH2 results in uterine hypertrophy and cystic endometrial hyperplasia in *Ezh2* cKO mice. Uterine weight (A) and size (B) were significantly greater in *Ezh2* cKO than WT mice at all ages measured. The inset shows data from PND 22 to allow the results to be more clearly visualized. Light areas (+) in B represent cystic endometrial hyperplasia. For the WT and *Ezh2*cKO uterine data shown in A and B, n = 4 and 8, respectively, at PND 22, 60, and 180. For both the WT and *Ezh2*cKO uteri at PND 60 and 180, respectively uterine data shown in A and B, n = 7 at PND 60 and n = 4 at PND 180, respectively. (C) By PND 120 in *Ezh2*cKO uteri, some uterine glands (G) had given rise to large endometrial cysts containing inflammatory cell infiltrates (inset). (D) Immunohistochemistry for FOXA2, an endometrial gland (arrows) marker, in ovariectomized WT and *Ezh2*cKO uteri at PND 74 revealed increased gland numbers in *Ezh2*cKO uteri. Similar increases were seen in intact *Ezh2*cKO compared to WT uteri (not shown). All whole mounts in B are at the same magnification, as are histological sections in panel D; the magnification bars = 2, 1, and 0.3 mm in B, C, and D, respectively. The n = 8 and 10 for the WT and *Ezh2*cKO uteri depicted in panel D. * = different than WT control at $P \leq 0.05$.

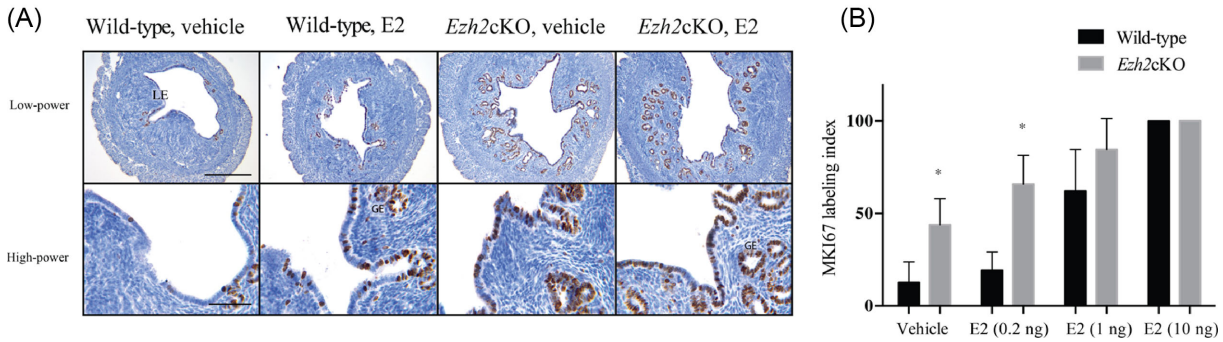

Figure 6. Loss of EZH2 results in ovary-independent luminal epithelial proliferation in *Ezh2*cKO uteri. Ovariectomized adult WT and *Ezh2*cKO mice (PND 74) were given oil or 0.2–10 ng/g BW 17β-estradiol (E2). Uteri were collected 24 h later and immunostained for MKI67, and luminal epithelial (LE) labeling indices (LI; labeled/total cells) were determined. (A) Proliferation in LE and glandular epithelium of oil-treated ovariectomized *Ezh2*cKO mice was sharply increased compared to oil-treated ovariectomized WT mice. Treatment of control and *Ezh2*cKO mice with 1 ng/g BW E2 further increased LE proliferation compared to vehicle-treated control and *Ezh2*cKO mice. All individual images in the top and bottom rows of panel A are at the same magnification, and the magnification bars = 0.3 and 0.1 mm in the top and bottom rows, respectively. (B) Uterine epithelial proliferation showed dose-responsive increases in WT and *Ezh2*cKO mice, with the maximal proliferation obtained at 10 ng/g BW E2 being comparable in WT and *Ezh2*cKO mice. An n of 3–6/group was used for MKI67 staining, and for uterine weights the n ranged from 4–8/group. * = different than WT at $P \leq 0.05$.

H3K27me3 presence in non-*Pgr* expressing cells. This could also reflect the ability of EZH1 (EZH2 homolog) to partly compensate for EZH2 loss [34]. RNA-seq analysis of WT and *Ezh2*cKO mice detected *Ezh1* mRNA expression in uteri of both WT and *Ezh2*cKO mice, although *Ezh1* mRNA expression did not show compensatory increases in *Ezh2*cKO uteri (unpublished data).

Our data indicated that uterine H3K27ac tended to increase in *Ezh2*cKO mice, potentially as a result of increases in histone acetyltransferases such as p300 or CBP, in contrast to decreased H3K27me3. The H3K27ac mark is associated with enhanced gene expression, and thus the *Ezh2*cKO uterine phenotype and aberrant uterine epithelial proliferation may reflect loss of repressive

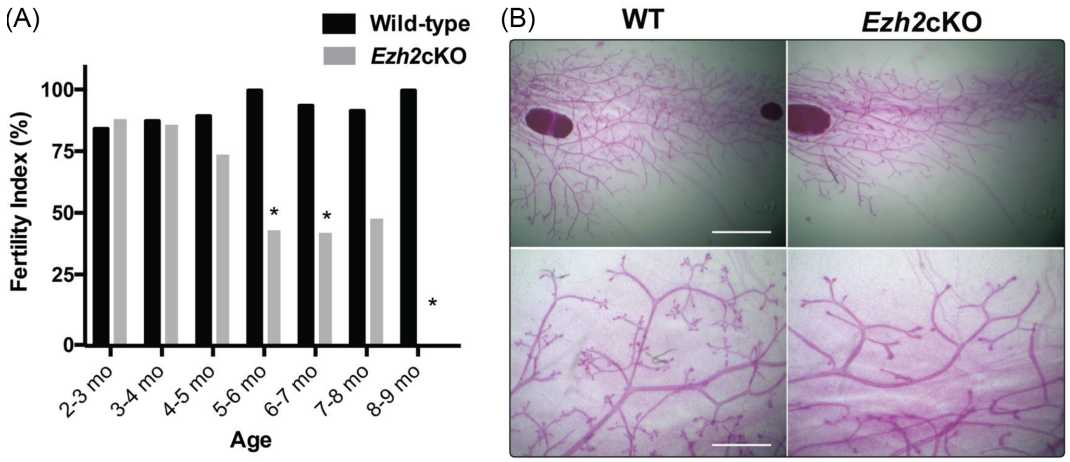

Figure 7. Fertility and mammary gland development are impaired in *Ezh2*cKO mice. (A) WT and *Ezh2*cKO females were paired with proven breeder males and subsequent births logged. For each age, females were considered fertile if they gave birth to a litter at that age or later. Litters were only counted if all pups were delivered with at least 1 pup alive. The n = 9–15 for *Ezh2*cKO mice between 2–3 months and 6–7 months of age, 6 for the 7–8 months of age and 5 for the 8–9 months of age. The n = 18–25 for groups of WT mice between 2–3 and 6–7 months of age, n = 12 for the 7–8 months of age and 6 for the 8–9 months of age. No births were noted for the *Ezh2*cKO mice (0/5) at 8–9 months of age or older. * = ages when *Ezh2* cKO fertility was less ($P \leq 0.05$) than WT. (B) Low- (top row) and high-power (bottom row) whole mounts of fourth mammary glands from WT and *Ezh2*cKO mice at PND 60. Magnification bars in top row = 5 mm, and in bottom row = 1 mm. A n of 4–5 was used for both groups.

Table 1. Litter size and pup survival in WT and *Ezh2*cKO females.

	Wild-type	*Ezh2*cKO
Litter size (at birth)	6.9 ± 0.3 (n = 95)	4.0 ± 0.4* (n = 43)
% survival to day 21	90 ± 3 (n = 77)	73 ± 7* (n = 34)

Litter numbers in the WT and *Ezh2*cKO females are shown in parentheses in the top row, and pup number for WT and *Ezh2*cKO females is shown in parentheses in the bottom row. * = different than WT at $P \leq 0.05$.

H3K27me3 marks as well as enhanced expression of some genes due to increased H3K27ac.

Increases in uterine size and weights in *Ezh2*cKO mice were seen by PND 22, and these increases became more pronounced with age. Increased uterine weight occurred without significant body weight changes. Uterine weight increases in *Ezh2*cKO mice resulted at least partly from increased epithelial proliferation and glandular fluid accumulation. There appears to be increased mitogenic responsivity to E2 in *Ezh2*cKO mice, shown by increased uterine epithelial proliferation at low E2 doses that did not increase WT uterine epithelial proliferation. However, the most significant contributor to uterine organomegaly may be ovary-independent uterine epithelial proliferation in *Ezh2*cKO mice. In striking contrast to WT mice, uterine epithelial proliferation was robust in oil-treated ovariectomized *Ezh2*cKO mice. Although uterine epithelium proliferated without E2, it also remained E2 responsive for proliferation, as illustrated by further dose-responsive increases in epithelial proliferation in E2-treated *Ezh2*cKO uteri.

In addition to well-known effects on transcriptional silencing through H3K27me3, EZH2 has other effects. EZH2 methylates nonhistone proteins and functions as a transcriptional co-activator to regulate genes in a PRC-2 independent manner (reviewed in [10]). Epigenetic changes induced by E2 at puberty may be essential for transitioning uterine epithelium from E2-independent neonatal proliferation to totally E2-dependent proliferation at puberty. Thus, *Ezh2*cKO uteri may remain less differentiated and show E2-independent epithelial proliferation characteristic of neonatal uteri, although these uteri remain E2-responsive and show further mitogenic responses to estrogen. These changes in *Ezh2*cKO mice likely reflect altered expression of many proteins in *Ezh2*cKO mice due to epigenetic changes, but the specific mechanism of this effect remains to be established. Although various transgenic mice exhibiting endometrial hyperplasia have been described [40–42], sometimes accompanied by estrogen-independent epithelial proliferation [42], our results indicate that knockout of proteins associated with histone modifications can produce such effects.

Uterine gland number was increased in ovariectomized *Ezh2*cKO mice, and E2 replacement induced especially intense proliferation in glandular epithelium. Increased mitogenic E2 responsiveness of glandular epithelium and the ability of glandular epithelium to proliferate and produce secretions even in ovariectomized *Ezh2*cKO mice may combine to produce the cystic endometrial hyperplasia characteristic of these mice at older ages. The increased proliferation of glandular epithelium may also contribute to uterine organomegaly in these mice.

Younger *Ezh2*cKO mice become pregnant and successfully raise pups despite altered uterine cell proliferation, although reproductive success was diminished, as judged by dystocia and decreased fertility, litter size, and pup survival. The ovary, oviduct, and some areas of the brain linked to reproduction express *Pgr*, suggesting that loss of EZH2 in tissues other than the uterus might be a factor in the decreased reproductive success of *Ezh2*cKO mice. However, our results show that that *Ezh2*cKO mice cycle normally and mate, as judged by the presence of copulation plugs, and that numbers of corpora lutea are normal in young *Ezh2*cKO mice. The number of implantation sites is normal in the *Ezh2*cKO mice that become pregnant, and uterine decidualization in these *Ezh2*cKO mice is comparable to WT. A significant fraction of *Ezh2*cKO mice do not become pregnant and lack implantation sites and decidualization despite the presence of normal numbers of corpora lutea in these animals. These results suggest that it is uterine abnormalities, perhaps in implantation or the initiation of decidualization, rather than neuroendocrine or ovarian problems that lead to the infertility in *Ezh2*cKO mice, although specific factors resulting in the lack of normal implantation in these mice remains to be determined. The less extensive mammary

gland development in *Ezh2*cKO mice could impair lactation and contribute to the decreased survival of pups from *Ezh2*cKO dams, although the normal weights and growth of surviving pups from *Ezh2*cKO females clearly indicate that these animals are capable of lactation.

Stimulatory effects on adult *Ezh2*cKO uteri contrast markedly with the mammary gland phenotype, which included decreased numbers of mammary end buds and less extensive ductal branching in these mice. These results are consistent with some, but not all, previous findings on EZH2 in mammary development. Initial studies suggested that mammary gland EZH2 knockdown or conditional knockout of EZH2 in mammary gland stem cells impaired terminal end bud formation, alveologenesis, and ductal elongation [18–20]. However, more recent work [20] using a mouse mammary tumor virus (MMTV)-driven cre recombinase that is expressed only in ductal cells suggested that conditional EZH2 knockout in mammary stem cells caused precocious and more extensive mammary ductal development. Our results strongly support initial studies suggesting EZH2 loss inhibits mammary development.

Previous studies using EZH2 conditional knockouts in several cell types produced varying changes. For example, Koike et al. [26] reported that conditional EZH2 deletion in liver reduced liver size and cell number, and impaired hepatic stem cell numbers and hepatocyte differentiation. Conditional EZH2 deletion in mouse intestine did not produce demonstrable effects, although conditional deletion of another protein involved in the PRC2 complex produced intestinal stem cell loss [37]. Feng et al. [27] reported that cerebellar EZH2 deletion caused transcriptional dysregulation and impaired differentiation of cerebellar cell types, resulting in cerebellar hypoplasia. Conditional deletion of EZH2 in early mesenchyme of mouse embryos led to skeletal deformities and reduced skeletal size [28], and conditional EZH2 knockout in mouse heart led to a constellation of cardiovascular abnormalities and perinatal death [29]. Differing phenotypes in various tissues following EZH2 deletion likely reflect tissue- and age-specific roles of EZH2. However, our results showing uterine hyperplasia and hypertrophy in *Ezh2*cKO mice contrast with previously reported conditional EZH2 knockouts in other tissues in that loss of uterine EZH2 can have stimulatory effects on organ size and growth.

In conclusion, uterine EZH2 expression shows age-dependent changes and is correlated with epithelial proliferation and regulated by sex steroid hormones. Loss of EZH2 alters uterine growth and histology, epithelial proliferation, and E2 responsiveness, and produces phenotypic changes dissimilar from other tissues where EZH2 was conditionally deleted. These changes, in conjunction with the concomitant impaired mammary gland phenotype, may account for impaired fertility and reduced postnatal pup survival in *Ezh2*cKO mice. Overall, EZH2 is required for normal uterine and mammary development and function. Further studies utilizing these mice may provide insights into the epigenetic landscape in developing uteri and mechanistic regulation of this process.

Conflict of Interest: The authors have declared that no conflict of interest exists.

Note added in proof: Following initial submission and review of our manuscript, Fang et al (Am J Pathol 189:1212-1225, 2019) also reported the development of a uterine conditional knockout of EZH2 and saw changes in uterine epithelial proliferation.

Supplementary data

Supplementary data are available at *BIOLRE* online.

Supplementary Table S1. Antibody table.

References

1. Jefferson WN, Kinyamu HK, Wang T, Miranda AX, Padilla-Banks E, Suen AA, Williams CJ. Widespread enhancer activation via ERα mediates estrogen response in vivo during uterine development. *Nucleic Acids Res* 2018; **46**:5487–5503.
2. Treviño LS, Wang Q, Walker CL. Phosphorylation of epigenetic "readers, writers and erasers": implications for developmental reprogramming and the epigenetic basis for health and disease. *Prog Biophys Mol Biol* 2015; **118**:8–13.
3. Grimaldi G, Christian M, Steel JH, Henriet P, Poutanen M, Brosens JJ. Down-regulation of the histone methyltransferase EZH2 contributes to the epigenetic programming of decidualizing human endometrial stromal cells. *Mol Endocrinol* 2011; **25**:1892–1903.
4. Jia N, Li Q, Tao X, Wang J, Hua K, Feng W. Enhancer of zeste homolog 2 is involved in the proliferation of endometrial carcinoma. *Oncol Lett* 2014; **8**:2049–2054.
5. Oki S, Sone K, Oda K, Hamamoto R, Ikemura M, Maeda D, Takeuchi M, Tanikawa M, Mori-Uchino M, Nagasaka K, Miyasaka A, Kashiyama T et al. Oncogenic histone methyltransferase EZH2: a novel prognostic marker with therapeutic potential in endometrial cancer. *Oncotarget* 2017; **8**:40402–40411.
6. Eskander RN, Tewari KS. Exploiting the therapeutic potential of the PI3K-AKT-mTOR pathway in enriched populations of gynecologic malignancies. *Expert Rev Clin Pharmacol* 2014; **7**:847–858.
7. Yoo KH, Hennighausen L. EZH2 methyltransferase and H3K27 methylation in breast cancer. *Int J Biol Sci* 2012; **8**:59–65.
8. Bae WK, Yoo KH, Lee JS, Kim Y, Chung IJ, Park MH, Yoon JH, Furth PA, Hennighausen L. The methyltransferase EZH2 is not required for mammary cancer development, although high EZH2 and low H3K27me3 correlate with poor prognosis of ER-positive breast cancers. *Mol Carcinog* 2015; **54**:1172–1180.
9. Varambally S, Dhanasekaran SM, Zhou M, Barrette TR, Kumar-Sinha C, Sanda MG, Ghosh D, Pienta KJ, Sewalt RGAB, Otte AP. The polycomb group protein EZH2 is involved in progression of prostate cancer. *Nature* 2002; **419**:624–629.
10. Gan L, Yang Y, Li Q, Feng Y, Liu T, Guo W. Epigenetic regulation of cancer progression by EZH2: from biological insights to therapeutic potential. *Biomark Res* 2018; **6**:10.
11. Colón-Caraballo M, Monteiro JB, Flores I. H3K27me3 is an epigenetic mark of relevance in endometriosis. *Reprod Sci* 2015; **22**:1134–1142.
12. Yang Q, Laknaur A, Elam L, Ismail N, Gavrilova-Jordan L, Lue J, Diamond MP, Al-Hendy A. Identification of polycomb group protein EZH2-mediated DNA mismatch repair gene MSH2 in human uterine fibroids. *Reprod Sci* 2016; **23**:1314–1325.
13. Yang Q, Nair S, Laknaur A, Ismail N, Diamond MP, Al-Hendy A. The polycomb group protein EZH2 impairs DNA damage repair gene expression in human uterine fibroids. *Biol Reprod* 2016; **94**:69.
14. Varghese BV, Koohestani F, McWilliams M, Colvin A, Gunewardena S, Kinsey WH, Nowak RA, Nothnick WB, Chennathukuzhi VM. Loss of the repressor REST in uterine fibroids promotes aberrant G protein-coupled receptor 10 expression and activates mammalian target of rapamycin pathway. *Proc Natl Acad Sci USA* 2013; **110**:2187–2192.
15. Greathouse KL, Bredfeldt T, Everitt JI, Lin K, Berry T, Kannan K, Mittelstadt ML, Ho SM, Walker CL. Environmental estrogens differentially engage the histone methyltransferase EZH2 to increase risk of uterine tumorigenesis. *Mol Cancer Res* 2012; **10**:546–557.
16. Bhan A, Hussain I, Ansari KI, Bobzean SAM, Perrotti LI, Mandal SS. Histone methyltransferase EZH2 is transcriptionally induced by estradiol as

well as estrogenic endocrine disruptors bisphenol-A and diethylstilbestrol. *J Mol Biol* 2014; **426**:3426–3441.
17. Doherty LF, Bromer JG, Zhou Y, Aldad TS, Taylor HS. In utero exposure to diethylstilbestrol (DES) or bisphenol-A (BPA) increases EZH2 expression in the mammary gland: an epigenetic mechanism linking endocrine disruptors to breast cancer. *HORM Cancer* 2010; **1**:146–155.
18. Michalak EM, Nacerddine K, Pietersen A, Beuger V, Pawlitzky I, Cornelissen-Steijger P, Wientjens E, Tanger E, Seibler J, van Lohuizen M, Jonkers J. Polycomb group gene Ezh2 regulates mammary gland morphogenesis and maintains the luminal progenitor pool. *Stem Cells* 2013; **31**:1910–1920.
19. Pal B, Bouras T, Shi W, Vaillant F, Sheridan JM, Fu N, Breslin K, Jiang K, Ritchie ME, Young M, Lindeman GJ, Smyth GK et al. Global changes in the mammary epigenome are induced by hormonal cues and coordinated by Ezh2. *Cell Rep* 2013; **3**:411–426.
20. Yoo KH, Oh S, Kang K, Hensel T, Robinson GW, Hennighausen L. Loss of EZH2 results in precocious mammary gland development and activation of STAT5-dependent genes. *Nucleic Acids Res* 2015; **43**:8774–8789.
21. Jefferson WN, Chevalier DM, Phelps JY, Cantor AM, Padilla-Banks E, Newbold RR, Archer TK, Kinyamu HK, Williams CJ. Persistently altered epigenetic marks in the mouse uterus after neonatal estrogen exposure. *Mol Endocrinol* 2013; **27**:1666–1677.
22. Bredfeldt TG, Greathouse KL, Safe SH, Hung MC, Bedford MT, Walker CL. Xenoestrogen-induced regulation of EZH2 and histone methylation via estrogen receptor signaling to PI3K/AKT. *Mol Endocrinol* 2010; **24**:993–1006.
23. Walker CL. Epigenomic reprogramming of the developing reproductive tract and disease susceptibility in adulthood. *Birth Defects Res A Clin Mol Teratol* 2011; **91**:666–671.
24. O'Carroll D, Erhardt S, Pagani M, Barton SC, Surani MA, Jenuwein T. The polycomb-group gene EZH2 is required for early mouse development. *Mol Cell Biol* 2001; **21**:4330–4336.
25. Koppens MA, Bounova G, Gargiulo G, Tanger E, Janssen H, Cornelissen-Steijger P, Blom M, Song JY, Wessels LF, van Lohuizen M. Deletion of polycomb repressive complex 2 from mouse intestine causes loss of stem cells. *Gastroenterology* 2016; **151**:684–697.e12 e612.
26. Koike H, Ouchi R, Ueno Y, Nakata S, Obana Y, Sekine K, Zheng YW, Takebe T, Isono K, Koseki H, Taniguchi H. Polycomb group protein Ezh2 regulates hepatic progenitor cell proliferation and differentiation in murine embryonic liver. *PLoS ONE* 2014; **9**:e104776.
27. Feng X, Juan AH, Wang HA, Ko KD, Zare H, Sartorelli V. Polycomb Ezh2 controls the fate of GABAergic neurons in the embryonic cerebellum. *Development* 2016; **143**:1971–1980.
28. Hemming S, Cakouros D, Codrington J, Vandyke K, Arthur A, Zannettino A, Gronthos S. EZH2 deletion in early mesenchyme compromises postnatal bone microarchitecture and structural integrity and accelerates remodeling. *FASEB J* 2017; **31**:1011–1027.
29. Chen L, Ma Y, Kim EY, Yu W, Schwartz RJ, Qian L, Wang J. Conditional ablation of EZH2 in murine hearts reveals its essential roles in endocardial cushion formation, cardiomyocyte proliferation and survival. *PLoS ONE* 2012; **7**:e31005.
30. Pedram A, Razandi M, Lewis M, Hammes S, Levin ER. Membrane-localized estrogen receptor α is required for normal organ development and function. *Dev Cell* 2014; **29**:482–490.
31. Nanjappa MK, Hess RA, Medrano TI, Locker SH, Levin ER, Cooke PS. Membrane-localized estrogen receptor 1 is required for normal male reproductive development and function in mice. *Endocrinology* 2016; **157**:2909–2919.
32. Nanjappa MK, Medrano TI, March AG, Cooke PS. Neonatal uterine and vaginal cell proliferation and adenogenesis are independent of estrogen receptor 1 (ESR1) in the mouse. *Biol Reprod* 2015; **92**:78.
33. Soyal SM, Mukherjee A, Lee KYS, Li J, Li H, DeMayo FJ, Lydon JP. Cre-mediated recombination in cell lineages that express the progesterone receptor. *Genesis* 2005; **41**:58–66.
34. Shen X, Liu Y, Hsu Y-J, Fujiwara Y, Kim J, Mao X, Yuan G-C, Orkin SH. EZH1 mediates methylation on histone H3 lysine 27 and complements EZH2 in maintaining stem cell identity and executing pluripotency. *Mol Cell* 2008; **32**:491–502.
35. El Zowalaty AE, Li R, Zheng Y, Lydon JP, DeMayo FJ, Ye X. Deletion of RhoA in progesterone receptor-expressing cells leads to luteal insufficiency and infertility in female mice. *Endocrinology* 2017; **158**:2168–2178.
36. Harshman SW, Chen MM, Branson OE, Jacob NK, Johnson AJ, Byrd JC, Freitas MA. Isolation and analysis of linker histones across cellular compartments. *J Proteomics* 2013; **91**:595–604.
37. Kelleher AM, Peng W, Pru JK, Pru CA, DeMayo FJ, Spencer TE. Forkhead box a2 (FOXA2) is essential for uterine function and fertility. *Proc Natl Acad Sci USA* 2017; **114**:E1018–E1026.
38. Plante I, Stewart MKG, Laird DW. Evaluation of mammary gland development and function in mouse models. *J Vis Exp* 2011; Jul 21;(53). pii: 2828.
39. Franco HL, Jeong JW, Tsai SY, Lydon JP, DeMayo FJ. In vivo analysis of progesterone receptor action in the uterus during embryo implantation. *Semin Cell Dev Biol* 2008; **19**:178–186.
40. Zukerberg LR, DeBernardo RL, Kirley SD, D'Apuzzo M, Lynch MP, Littell RD, Duska LR, Boring L, Rueda BR. Loss of cables, a cyclin-dependent kinase regulatory protein, is associated with the development of endometrial hyperplasia and endometrial cancer. *Cancer Res* 2004; **64**:202–208.
41. Daikoku T, Yoshie M, Xie H, Sun X, Cha J, Ellenson LH, Dey SK. Conditional deletion of Tsc1 in the female reproductive tract impedes normal oviductal and uterine function by enhancing mTORC1 signaling in mice. *Mol Hum Reprod* 2013; **19**:463–472.
42. Gao Y, Li S, Li Q. Uterine epithelial cell proliferation and endometrial hyperplasia: evidence from a mouse model. *Mol Hum Reprod* 2014; **20**:776–786.